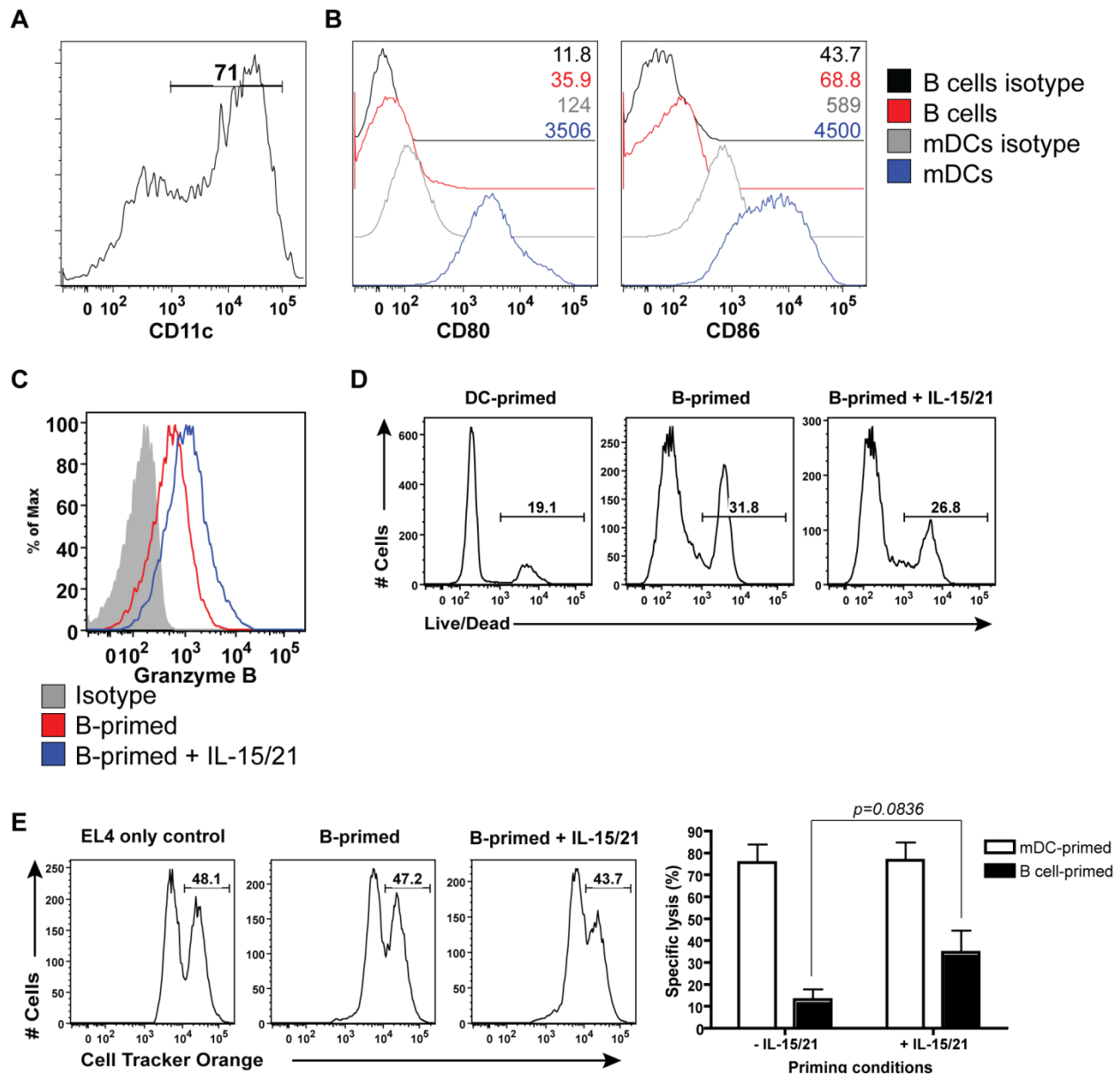


Supplemental Materials:

Detector	P.Value_DC/B	DDCt_DC-B	Log10RQ_DC-B	Fold Change (DC/B)
miR-298	0.00025	2.997	-0.902	0.125
miR-183	0.00120	2.864	-0.862	0.137
miR-520b	0.00314	-1.295	0.390	2.453
miR-200a	0.00617	-1.376	0.414	2.596
miR-25	0.01029	1.480	-0.446	0.358
miR-500	0.01050	-0.440	0.132	1.356
miR-323-5p	0.01551	-0.673	0.203	1.594
miR-23a	0.01595	3.424	-1.031	0.093
miR-7a	0.01759	1.414	-0.426	0.375
miR-424*	0.02121	-1.873	0.564	3.663
miR-15a*	0.02289	0.347	-0.104	0.786
miR-677	0.02749	3.240	-0.975	0.106
miR-675-5p	0.03095	1.344	-0.404	0.394
miR-92b	0.03641	1.787	-0.538	0.290
miR-23b	0.04292	3.120	-0.939	0.115
miR-487b	0.04670	2.100	-0.632	0.233
miR-20b	0.04698	0.867	-0.261	0.548
miR-421	0.04833	3.560	-1.072	0.085

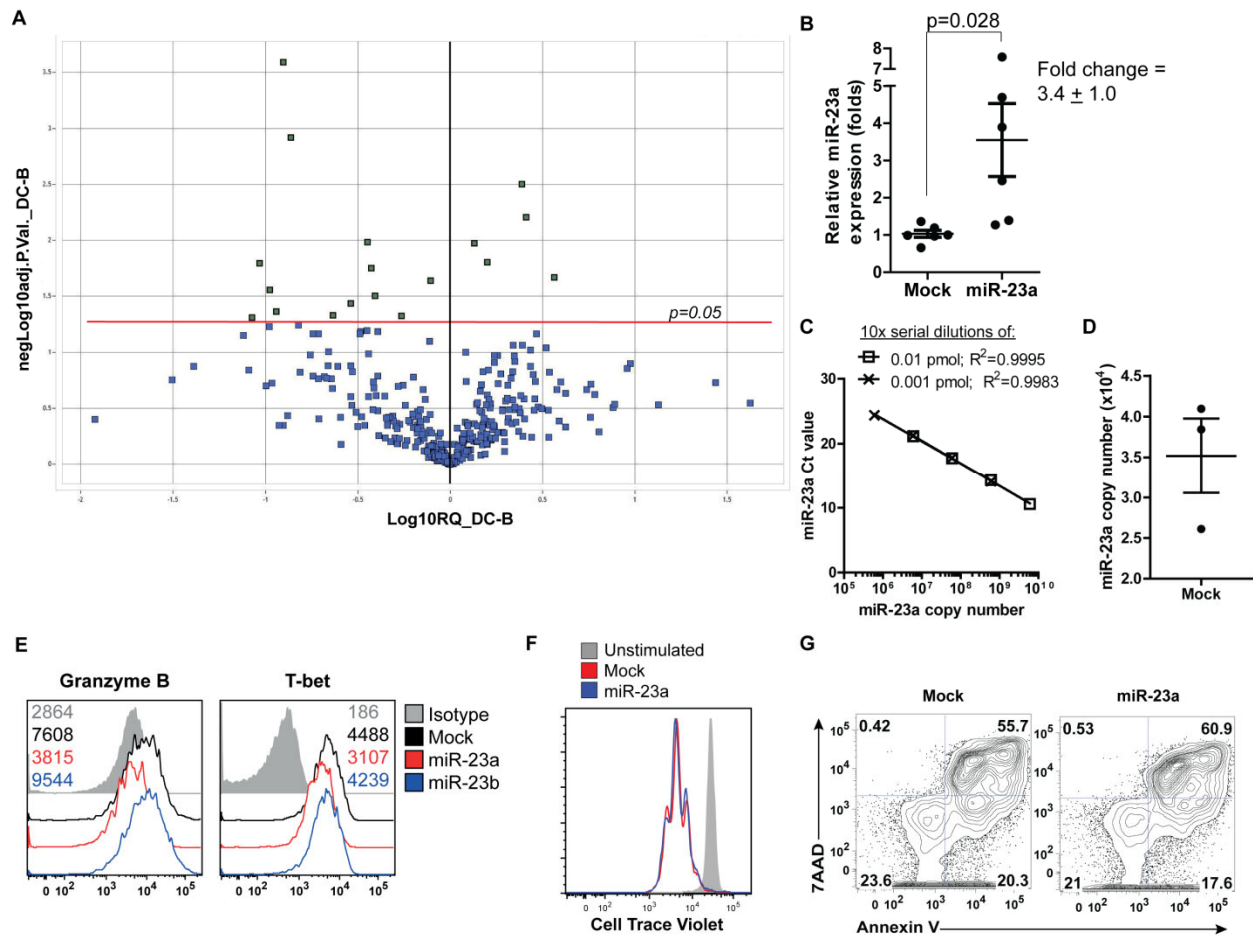
Supplemental Table 1: 18 miRNAs significantly differentially expressed in DC- and B cell-primed CTLs, as determined by the paired t-test with significance level set at 0.05.



Supplemental Figure 1: *In vitro* priming system for generating CTLs with different cytotoxic abilities. (A and B) Phenotype of splenic B cells and LPS-matured BMDCs (mDCs) used for naïve CTL priming *in vitro*. (A) CD11c expression on LPS-matured BMDCs. (B) Surface expression of CD80 and CD86 on splenic B cells and mDCs. Numbers within histograms indicate mean fluorescence intensity. (C-E) Exogenous IL-15 and IL-21 protect B cell-primed CTLs from activation-induced cell death (AICD) and enhance granzyme B expression, but fail to

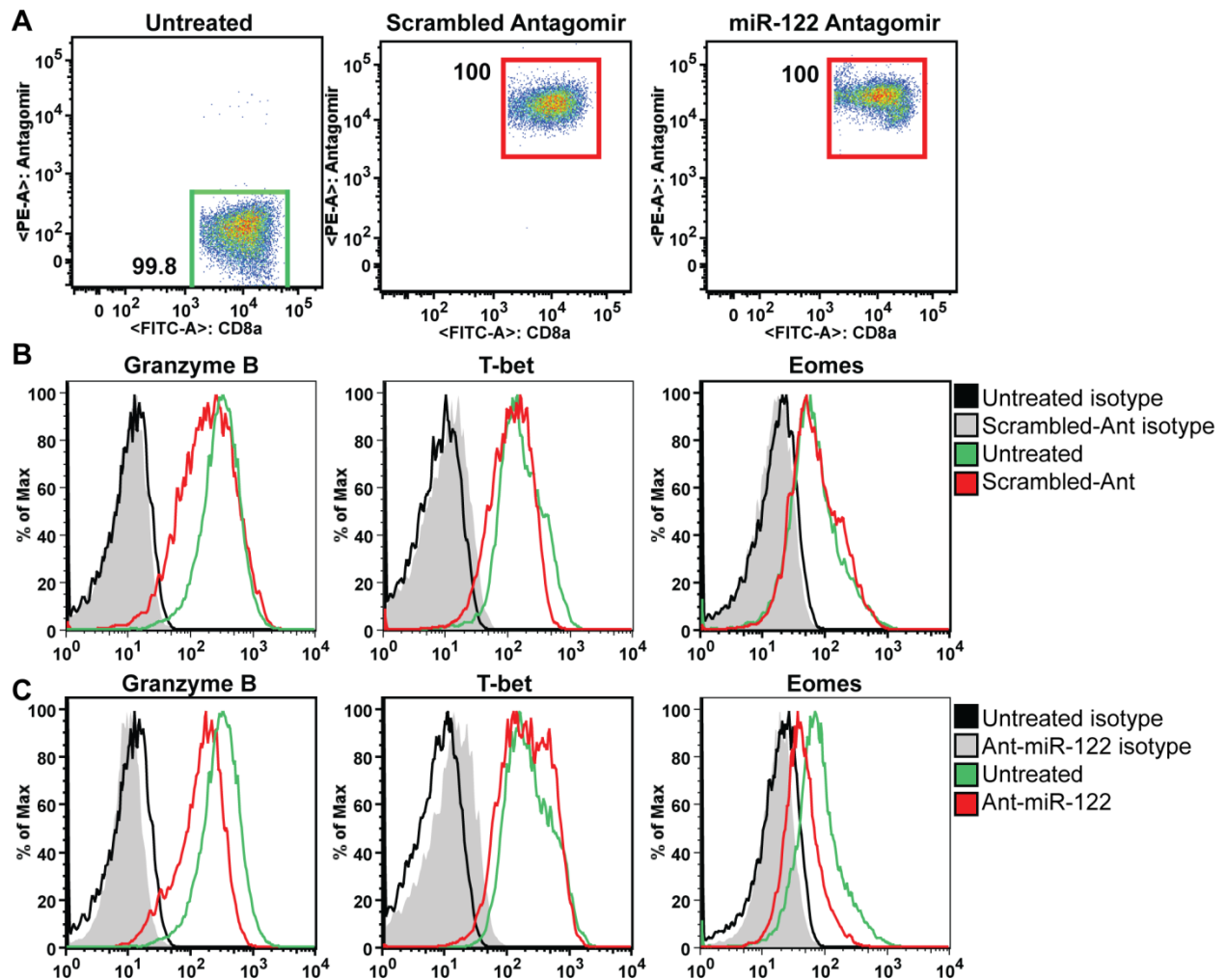
increase cytotoxicity *in vitro*. (C) Granzyme B expression in CTLs primed with B cells in the absence or presence of IL-15 and IL-21. (D and E) pMel-1 CTLs primed with mDCs, B cells or B cells in the presence of IL-15 and IL-21 were incubated for 6 hours with peptide-pulsed EL4 target cells, and assessed for (D) AICD of CD8⁺ CTLs, and (E) *in vitro* cytotoxicity.

Representative histograms and bar graph depicting Mean \pm S.E.M. from n=3 independent experiments.

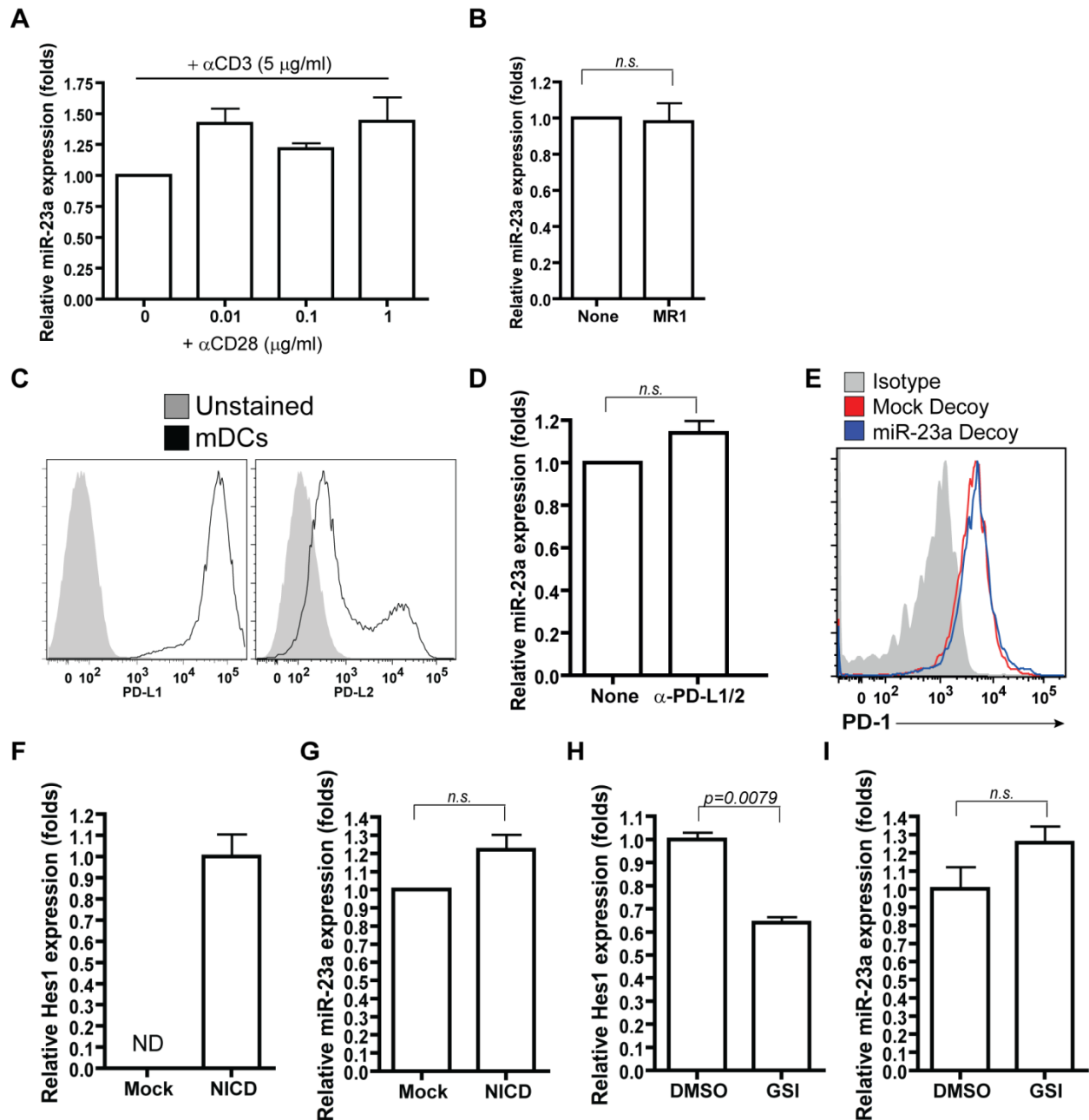


Supplemental Figure 2: Identification of miR-23a as a negative correlate of CTL effector function. (A) Volcano plot of miRNA expression profiling. The 18 miRNAs significantly differentially-expressed in DC- and B cell-primed CTLs are indicated in green; red line indicates $p=0.05$. (B-E) pMel-1 CTLs were retrovirally-transduced with a Mock vector, the miR-23a overexpression vector or the miR-23b overexpression vector. (B) miR-23a overexpression levels in CTLs 4 days post-transduction from $n=6$ independent samples. (C) Chemically-synthesized miR-23a was serially diluted to generate a standard curve for miR-23a copy number determination. Linear regression was conducted and the R^2 coefficients are shown. (D) miR-23a copy number in Mock-transduced pMel-1 CTLs from (B). (E) Granzyme B and T-bet expression in transduced pMel-1 CTLs. 4 to 6 days post-transduction, Mock and miR-23a-overexpressing

TCR β +GFP+ pMel-1 CTLs were restimulated for (F) 48 hours to assess cell proliferation or (G) 72 hours to assess AICD.

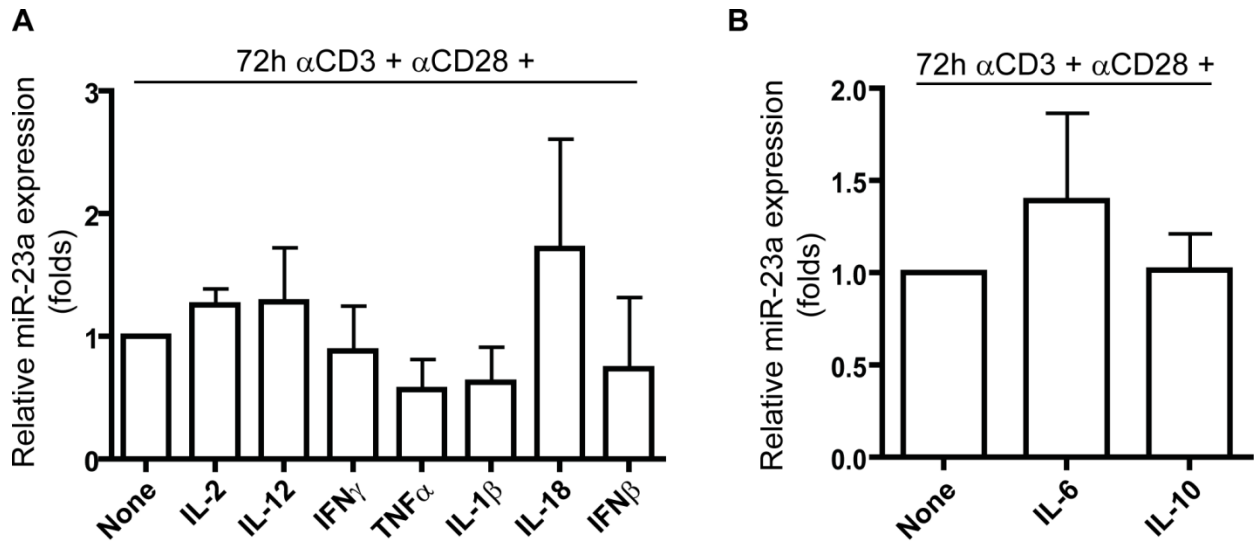


Supplemental Figure 3: Inhibiting miRNAs unrelated to miR-23a do not enhance CTL effector function. Purified naïve pMel-1 CTLs were activated with anti-CD3/anti-CD28 for 48h *in vitro*, in the presence or absence of 50 µg/ml PE-tagged scrambled antagomir, or the unrelated miR-122 antagomir. (A) Gating strategy to identify Antagomir+ CTLs. Note all CTLs were Antagomir+, indicating saturating amounts of antagomirs. Expression of effector molecules in CD8+ CTLs treated with (B) scrambled antagomir and (C) miR-122 antagomir were assessed by flow cytometry, and compared to their untreated counterparts. Data shown is one representative of three independent experiments.

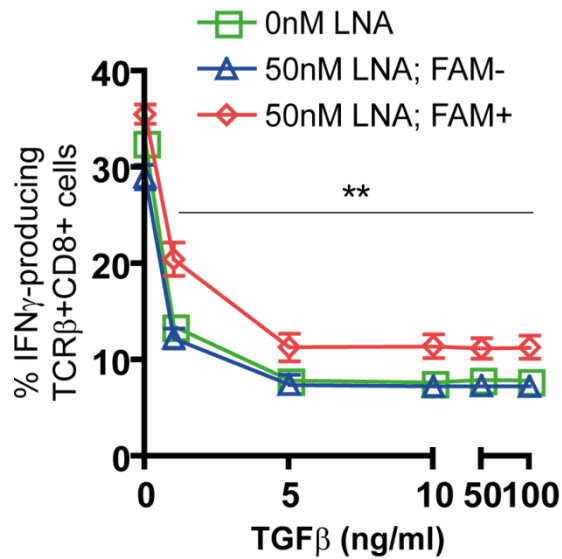


Supplemental Figure 5: Influence of receptor:ligand interactions at the T:APC interface on miR-23a expression in CTLs. (A-E) Co-receptor signaling through CD28, CD40L and PD-1 do not affect miR-23a expression in CTLs. (A) Purified naïve CTLs were activated *in vitro* with 5 μ g/ml α CD3 and the indicated concentrations of α CD28 (μ g/ml). Statistical analysis was performed by two-way ANOVA with Bonferroni post-test. (B) Naïve CTLs were primed *in vitro*

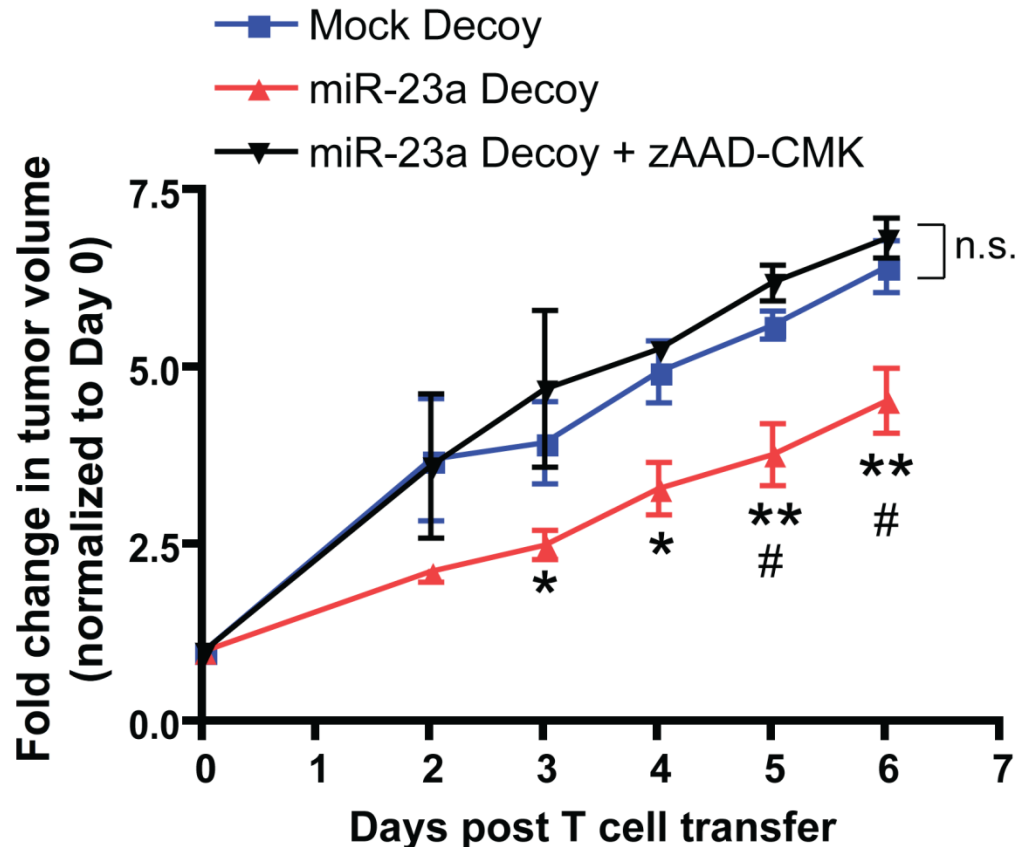
with mDCs, in the presence of blocking antibodies against CD40L on T cells (MR1 antibody). (C) mDCs express the PD-1 ligands, PD-L1 and PD-L2. (D) Naïve CTLs were primed *in vitro* with mDCs, in the presence of blocking antibodies against PD-1 ligands (α -PD-L1 and α -PD-L2) on mDCs. After 3 days of priming, CTLs were purified for miR-23a expression analysis by qPCR. (E) miR-23a inhibition does not affect PD-1 expression on CTLs. CD8⁺iRFP⁺GFP⁺ pMel-1 CTLs transduced with the Mock or miR-23a decoy vector were assessed for surface expression of PD-1. (F-I) Notch signaling does not regulate miR-23a expression in CTLs. (F and G) Notch activation was enforced in B cell-primed pMel-1 CTLs by transduction with a retroviral vector encoding the Notch intracellular domain (NICD), enabling constitutive activation of the Notch pathway. 4 to 6 days post-transduction, TCR β ⁺GFP⁺ pMel-1 CTLs were sorted for analysis of (F) mRNA expression of the Notch target gene Hes1; and (G) miR-23a expression. (H and I) Notch signaling was inhibited in mDC-primed pMel-1 CTLs by treatment with a γ -secretase inhibitor (GSI). After 3 days of *in vitro* priming, TCR β ⁺ pMel-1 CTLs were isolated and assessed for (H) Hes1 mRNA expression and (I) miR-23a expression. Data shown in (A) represent Mean \pm S.E.M. from n=3 independent experiments and data shown in (B-I) represent Mean \pm S.E.M. from n=2 independent experiments. ND: not detectable. Statistical significance in (B, D, G-I) was determined by the two-tailed paired t-test.



Supplemental Figure 6: Cytokines that do not alter miR-23a expression in CTLs. Purified naïve CTLs were activated with α CD3 and α CD28, in the presence of the indicated (A) inflammatory cytokines and (B) tumor-associated cytokines. After 3 days, CTLs were assessed for miR-23a expression. Data shown represents Mean \pm S.E.M. from $n \geq 2$ independent experiments. Statistical analysis was performed by one-way ANOVA with Bonferroni post-test.



Supplemental Figure 7: miR-23a inhibition in CTLs enhances the acquisition of IFN γ expression, even in the presence of TGF β . Purified naïve pMel-1 CTLs were activated with anti-CD3/anti-CD28 and the indicated concentrations of TGF β for 48h *in vitro*, in the presence or absence of 50nM FAM-tagged anti-miR-23a LNA. The percentage of IFN γ -producing TCR β +CD8+FAM- and TCR β +CD8+FAM+ cells were assessed by flow cytometry. Data shown represents Mean \pm S.E.M. of n=8 independent experiments. **p<0.01 for 50nM LNA FAM+ VS both 0nM LNA and 50nM LNA FAM- by two-way ANOVA and Bonferroni post-test.



Supplemental Figure 8: Inhibiting granzyme B in pMel-1 CTLs abrogates the therapeutic advantage conferred by the miR-23a Decoy. On Day 0, mice bearing large, established B16/F10 melanoma ($>1000 \text{ mm}^3$) received intratumoral injections of 0.2×10^6 Mock Decoy pMel-1 CTLs, 0.2×10^6 miR-23a Decoy pMel-1 CTLs or 0.2×10^6 miR-23a Decoy pMel-1 CTLs pre-treated with the granzyme B inhibitor zAAD-CMK. An additional 10 μg zAAD-CMK, or DMSO vehicle control, was injected intratumorally into each mouse on Day 3. Tumor volumes were normalized to that of Day 0, prior to the initiation of CTL therapy. Data represent Mean \pm S.E.M. from $n=4$ (miR-23a Decoy + zAAD-CMK) or $n=5$ (Mock Decoy and miR-23a Decoy) mice per group. # $p<0.05$ and 0.01 for miR-23a Decoy VS Mock Decoy; * $p<0.05$ and ** $p<0.01$ for miR-23a Decoy VS miR-23a Decoy + zAAD-CMK by two-way ANOVA and Bonferroni post-test.